Generalized asymptotic description of the propagated field dynamics in Gaussian pulse propagation in a linear, causally dispersive medium

Constantinos M. Balictsis*
Department of Computer Science & Electrical Engineering, University of Vermont, Burlington, Vermont 05405

Kurt E. Oughstun
College of Engineering & Mathematics, University of Vermont, Burlington, Vermont 05405

(Received 22 February 1996)

As the initial pulse envelope width of an input Gaussian pulse-modulated harmonic wave is increased above the characteristic relaxation time of a single resonance Lorentz model dielectric, the classical asymptotic description of the propagated field becomes increasingly inaccurate at a fixed propagation distance and must then be generalized in order to become uniformly valid with respect to the initial pulse width. The required generalization results in a modified complex phase function that depends not only upon the dispersive medium parameters and the propagation distance, but also upon the initial pulse width. The resultant modified asymptotic description of Gaussian pulse propagation is shown to be uniformly valid in the initial pulse width. The modified asymptotic description presented here reduces to the classical asymptotic result presented in an earlier paper [Phys. Rev. E **47**, 3645 (1993)] in the limit of an input ultrashort Gaussian pulse. In the opposite limit of a very broad input pulse, the modified asymptotic description reduces to that obtained with the well-known quasimonochromatic or slowly varying envelope approximation. Furthermore, the modified asymptotic description provides a clear description of the transition from the ultrashort limit to the quasimonochromatic regime for Gaussian pulse propagation. [S1063-651X(97)01702-9]

PACS number(s): 03.40.Kf

I. INTRODUCTION

Recently developed pulse generation and compression techniques have enabled the production of ultrashort electromagnetic wave packets in a variety of spectral domains, such as the far-infrared [1] and visible [2] regions, which contain only a few oscillation periods under their envelope. The advent of such ultrashort pulses has since posed critical questions on the validity of the slowly varying envelope approximation which is commonly utilized to describe their propagation in linear [3–5] as well as nonlinear [4–7] dispersive media. This is due to the violation of the basic assumption in this approximation concerning the slow variation of the complex pulse envelope over its average oscillation period and over its average wavelength [5]. An important alternative towards overcoming this critical difficulty in linear, causally dispersive media originated with the seminal investigations of Sommerfeld and Brillouin [8], who used the asymptotic method of steepest descents [9,10] in order to describe the propagation of a unit step-function-modulated harmonic wave in a single resonance Lorentz model dielectric. More recently, use of modern asymptotic techniques [10–15] has substantially improved the analytic description of the solution to this important canonical propagation problem [16–19] whose accuracy has been completely verified through comparison with purely numerical experiments [19–22]. Moreover, use of these asymptotic techniques has also led to an accurate, uniformly valid description of the dynamical evolution of the propagated field due to an input δ function pulse [16,17,19] and, more importantly, due to an input rectangular-envelope-modulated harmonic wave of arbitrary initial pulse width [18,23,24] in a single as well as a multiple resonance Lorentz medium.

Subsequent attempts to extend these modern asymptotic techniques to the canonical problem of Gaussian pulse propagation have, until now, been restricted to the extreme ultrashort pulse regime where pulse breakup into generalized precursor fields is observed [18,24,25]. On the other hand, the majority of approaches to this important canonical problem have been restricted to relatively broad input pulses [26] due to their reliance on the slowly varying envelope approximation [27–36]. In this paper we present an asymptotic description of the propagated field dynamics for Gaussian pulse propagation of arbitrary initial pulse width in a single resonance Lorentz model dielectric. This analysis is based upon a modified asymptotic approach [37–39] that utilizes the saddle point method due to Olver [10,11] and results in an asymptotic description of the propagated field which reduces to the opposite limiting descriptions afforded by the previous approaches which are only applicable either in the extreme ultrashort or else in the slowly varying envelope pulse regimes.

II. INTEGRAL FORMULATION OF GAUSSIAN PULSE PROPAGATION

Consider an input unit-amplitude, Gaussian-envelope-modulated harmonic wave of constant applied carrier frequency $\omega_c > 0$ and initial pulse width (full width at the e^{-1} points) $2T > 0$ that is given by

*Present address: M&S Hourdakis SA Electronics, R&D Department, Industrial Area Koropi, P.O. Box 117, 19400 Koropi, Attiki, Greece.

$$f(t)=\exp\left\{-\left(\frac{t-t_0}{T}\right)^2\right\}\sin(\omega_c t+\psi), \tag{1}$$

which is propagating in the positive z direction through a linear, homogeneous, isotropic, temporally dispersive dielectric whose frequency dispersion is described by the single resonance Lorentz model with complex index of refraction

$$n(\omega)=\left(1-\frac{b^2}{\omega^2-\omega_0^2+2i\delta\omega}\right)^{1/2}, \tag{2}$$

which occupies the source-free half space $z\geqslant 0$. Here ω_0 is the undamped resonance frequency, δ the phenomenological damping constant, and b is the plasma frequency of the lossy, dispersive dielectric. The input Gaussian envelope at the plane $z=0$ is centered around the time $t_0>0$ and is considered to extend over all time. Moreover, the constant phase factor ψ appearing in Eq. (1) is equal to zero for a modulated sine wave while it is equal to $\pi/2$ for a modulated cosine wave. The integral representation of the propagated plane wave pulse in the half space $z\geqslant 0$ is given by

$$A(z,t)=\frac{1}{2\pi}\int_c \tilde{f}(\omega)\exp\left[\frac{z}{c}\phi(\omega,\theta)\right]d\omega, \tag{3}$$

where $\theta=ct/z$ is a dimensionless space-time parameter, $\phi(\omega,\theta)=i\omega[n(\omega)-\theta]$ is the classical complex phase function, and where

$$\tilde{f}(\omega)=\int_{-\infty}^{\infty} f(t)e^{i\omega t}dt, \tag{4}$$

is the temporal Fourier spectrum of the initial pulse $f(t)=A(0,t)$ at the plane $z=0$. Here $A(z,t)$ represents either the scalar potential or any scalar component of the electric field, magnetice field, Hertz vector, or vector potential field whose spectral amplitude $\tilde{A}(z,\omega)$ satisfies the scalar Helmholtz equation

$$[\nabla^2+\tilde{k}^2(\omega)]\tilde{A}(z,\omega)=0, \tag{5}$$

which is said to be dispersive. The complex wave number $\tilde{k}(\omega)$ is given by

$$\tilde{k}(\omega)=\beta(\omega)+i\alpha(\omega)=\frac{\omega}{c}n(\omega), \tag{6}$$

where c denotes the speed of light in vacuum. Here $\beta(\omega)=\mathrm{Re}\{\tilde{k}(\omega)\}$ is the plane wave propagation factor and $\alpha(\omega)=\mathrm{Im}\{\tilde{k}(\omega)\}$ is the attenuation factor, where Re{ } denotes the real part and Im{ } the imaginary part of the quantity appearing inside the braces.

The classical asymptotic description of ultrashort Gaussian pulse propagation presented in Ref. [25], which consists of an application of modern asymptotic methods of approximation to the classical integral representation (3) of Gaussian pulse propagation, is incapable of providing an accurate description of the propagated field dynamics when the initial pulse width $2T$ of the input Gaussian pulse-modulated time harmonic wave is increased above the characteristic relaxation time $1/\delta$ of the lossy, dispersive medium under consideration. In order to overcome this problem and obtain an approximation of the propagated field which is uniformly valid not only in space and time but also in the initial pulse width $2T$, the classical integral formulation of Gaussian pulse propagation is rewritten as the *exact, modified integral representation of the propagated field* $A(z,t)$, which is given by [37–39]

$$A(z,t)=\frac{1}{2\pi}\mathrm{Re}\left\{i\int_c \tilde{U}_M\exp\left[\frac{z}{c}\Phi_M(\omega,\theta')\right]d\omega\right\} \tag{7a}$$

for all $z\geqslant 0$, where the modified complex spectral amplitude $\tilde{U}_M$ for the Gaussian-envelope pulse is independent of the angular frequency ω and is given by

$$\tilde{U}_M=\pi^{1/2}T\exp[-i(\omega_c t_0+\psi)], \tag{7b}$$

and where the modified complex phase function $\Phi_M(\omega,\theta')$ is given by

$$\Phi_M(\omega,\theta')=i\omega[n(\omega)-\theta']-\frac{cT^2}{4z}(\omega-\omega_c)^2. \tag{7c}$$

Here

$$\theta'=\frac{c}{z}(t-t_0)=\theta-\frac{ct_0}{z} \tag{8}$$

is a dimensionless space-time parameter which characterizes any specific space-time point in the propagated field evolution. The contour of integration C appearing in Eq. (7a) may be taken either as the real frequency axis or as any other contour in the complex ω plane that is homotopic to this axis. Moreover, the first term appearing on the right-hand side of Eq. (7c) is the classical complex phase function $\phi(\omega,\theta')$, while the second term appearing on the right-hand side of that equation is a complex phase term $\Phi_f(\omega)$ that is due to the frequency spectrum of the input Gaussian pulse. Notice that for any finite, fixed input pulse width $2T>0$, the modified phase function $\Phi_M(\omega,\theta')$ approaches the classical phase function $\phi(\omega,\theta')$ as the propagation distance z increases. Hence, at a sufficiently large propagation distance, the propagated field behavior will reduce to that given by the classical asymptotic description [24,25].

Although $\phi^*(-\omega^*,\theta')=\phi(\omega,\theta')$, where the superscript asterisk denotes the complex conjugate, because of the second term in the definition (7c) of the modified phase function,

$$\Phi_M^*(-\omega^*,\theta')\neq\Phi_M(\omega,\theta'), \tag{9}$$

and the modified complex phase function is not symmetric about the imaginary frequency axis. Nevertheless, as with the case of the classical complex phase function $\phi(\omega,\theta')$, both the modified complex phase function $\Phi_M(\omega,\theta')$ and the complex index of refraction $n(\omega)$ are analytic everywhere in the complex ω plane except at the four branch points $\omega'_{\pm}$ and $\omega_{\pm}$ of $n(\omega)$, where

$$n(\omega)=\left[\frac{(\omega-\omega'_+)(\omega-\omega'_-)}{(\omega-\omega_+)(\omega-\omega_-)}\right]^{1/2} \tag{10}$$

for a single resonance Lorentz model dielectric, with

$$\omega'_{\pm} = \pm\sqrt{\omega_1^2 - \delta^2} - i\,\delta, \tag{11a}$$

$$\omega_{\pm} = \pm\sqrt{\omega_0^2 - \delta^2} - i\,\delta, \tag{11b}$$

where $\omega_1^2 = \omega_0^2 + b^2$. The Lorentz model is a causal model [3] of dielectric dispersion that has played a central role in the rigorous analysis of dispersive pulse propagation phenomena [8,16,17,40]. The medium parameters that were originally chosen by Brillouin [8] and have been used in recent research [16–18, 23–25, 40] are used in the examples presented in this paper, viz., $\omega_0 = 4\times 10^{16}$ sec^{-1}, $b^2 = 20\times 10^{32}$ sec^{-2}, and $\delta = 0.28\times 10^{16}$ sec^{-1}. These medium parameters correspond to a highly absorptive medium.

III. UNIFORM ASYMPTOTIC DESCRIPTION OF GAUSSIAN PULSE PROPAGATION

At each value of θ', an application of the modern asymptotic approach to the modified integral representation given in Eq. (7a) results in a uniformly valid description of the propagated pulse dynamics that is given by the general expression [37,39]

$$A(z,t) = \sum_k A_{Mk}(z,t), \tag{12a}$$

where each term $A_{Mk}(z,t)$ represents a separate asymptotic contribution to the propagated field $A(z,t)$ that is given by

$$A_{Mk}(z,t) = \left(\frac{c}{2\pi z}\right)^{1/2} \mathrm{Re}\left\{ i \exp\left[\frac{z}{c}\Phi_M(\omega_{P_{Mk}}, \theta')\right] \times \frac{\widetilde{U}_M}{[-d^2\Phi_M(\omega_{P_{Mk}}, \theta')/d\omega^2]^{1/2}}[1 + O(z^{-1})]\right\}, \tag{12b}$$

as $z\to\infty$. The summation index k appearing in Eq. (12a) refers only to those saddle points P_{Mk} of the modified phase function $\Phi_M(\omega,\theta')$ that are relevant [37,39] at the particular value of θ' under consideration; their respective locations in the complex ω plane are denoted by $\omega_{P_{Mk}}(\theta')$. From Eq. (12b), each component field $A_{Mk}(z,t)$ is due to the asymptotic contribution of the respective relevant saddle point P_{Mk} to the uniform asymptotic approximation of the modified integral representation (7a) of the propagated field. In the derivation of Eqs. (12a) and (12b) the relevant saddle points of $\Phi_M(\omega,\theta')$ are considered to be isolated from each other and of first order at each value of θ', and only the first term in the asymptotic expansion about each of these saddle points has been retained. Each of these simplications is completely justified for a single resonance Lorentz model dielectric.

From Eqs. (12a) and (12b) and the results of the Appendix, the dynamical evolution of the propagated field due to an input Gaussian-envelope-modulated harmonic wave of arbitrary initial pulse width at a fixed, but otherwise arbitrary, propagation distance in the mature dispersion region of a linear, causally dispersive medium whose frequency dispersion is described by the single resonance Lorentz model, is dominated over any particular time interval by the pulse component that is due to the asymptotic contribution of the dominant, relevant saddle point of the modified phase function over this same time interval. The propagation characteristics of each such dominant pulse component of the propagated field are described by the dynamics of the respective dominant relevant saddle point over the corresponding time interval. In particular, the following four propositions are found to be valid.

Proposition 1. From Eq. (A4), the temporal evolution of the instantaneous angular frequency of oscillation of each dominant pulse component is given by the real part of the location of the respective dominant, relevant saddle point as it evolves with time in the complex ω plane.

Proposition 2. From Eqs. (A6)–(A9), the envelope of any given dominant pulse component attains a stationary point when the trajectory followed by the corresponding dominant, relevant saddle point intersects the real frequency axis in the complex ω plane. From Eqs. (12b) and (A11), this point of intersection is also a stationary point of the real part of the modified complex phase function along the real frequency axis and is a maximum (minimum) if the corresponding stationary point of the envelope of that pulse component is also a maximum (minimum).

Proposition 3. From Eqs. (A16a) and (A16b), the propagation velocity of a stationary point of the envelope of a dominant pulse envelope is equal to the classical group velocity evaluated at the instantaneous angular frequency of oscillation associated with this stationary point.

Proposition 4. Finally, from Eq. (A13), if the instantaneous oscillation frequency of a stationary point of the envelope of a dominant pulse component of the propagated field is equal to the applied carrier frequency ω_c of the input pulse, then the absorption coefficient of the dispersive medium attains a stationary point at this carrier frequency. This stationary point is a maximum (minimum) if the corresponding stationary point of the envelope of the respective pulse component is a minimum (maximum).

For the single resonance Lorentz model dielectric that is of central interest here, both analytical and numerical investigations have revealed [37,39] that the modified complex phase function $\Phi_M(\omega,\theta')$ possesses five first-order saddle points P_{Mk}, $k=1,2,\ldots,5$. As the space-time parameter θ' increases over its entire domain, only each of the two saddle points P_{Ml}, $l=1,2$, whose main dynamical evolution occurs in the first quadrant of the complex ω plane ($\omega_r \geqslant 0$, $\omega_i \geqslant 0$), can become a dominant, relevant saddle point over its corresponding θ' interval $\Delta\theta_{Ml}$. The asymptotic behavior of the propagated field $A(z,t)$ is then dominated by the respective pulse component $A_{Ml}(z,t)$, $l=1,2$, in each corresponding θ' interval. Moreover, it was found

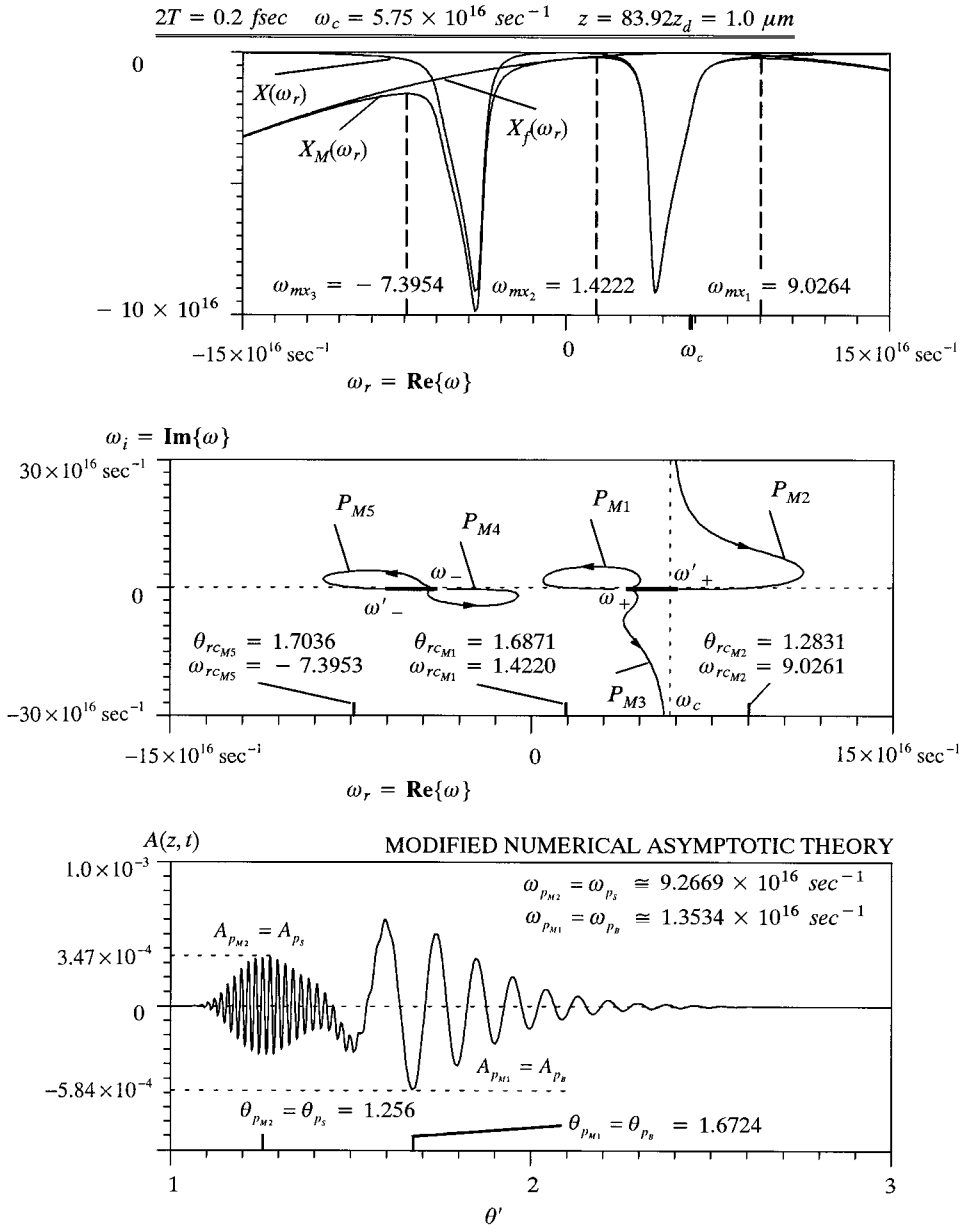

FIG. 1. Asymptotic description of the dynamical field structure due to an input ultrashort Gaussian-modulated cosine wave with initial pulse width $2T = 0.2$ fsec and applied carrier frequency $\omega_c = 5.75\times10^{16}$ sec^{-1} at a propagation distance of 83.92 absorption depths at that carrier frequency. The upper diagram illustrates the frequency dependence of the real part of the modified complex phase function along the real frequency axis, the middle diagram illustrates the dynamical evolution in the complex ω plane of the five saddle points of the modified phase function as a function of the space-time parameter θ', and the bottom diagram illustrates the dynamical evolution of the propagated pulse at the prescribed propagation distance in the single resonance Lorentz model dielectric.

[37,39] that in each θ' interval $\Delta\theta_{Ml}$, $l=1,2$, the envelope of the corresponding dominant pulse component $A_{Ml}(z,t)$ is Gaussian shaped with a single stationary point that is a maximum. From Eq. (12b), the value of the pulse component $A_{Ml}(z,t)$ at its associated stationary point is given by

$$A_{p_{Ml}} = \left(\frac{c}{2\pi z}\right)^{1/2} \mathrm{Re}\left\{ i\tilde{U}_M \exp\left[\frac{z}{c}\Phi_M(\omega_{p_{Ml}}, \theta_{p_{Ml}})\right] \times \left[-\frac{d^2\Phi_M(\omega_{p_{Ml}}, \theta_{p_{Ml}})}{d\omega^2}\right]^{-1/2} [1+O(z^{-1})]\right\}, \tag{13}$$

as $z\to\infty$, for $l=1,2$, where $\theta_{p_{Ml}}$ and $\omega_{p_{Ml}}$ are defined in Eqs. (A10a) and (A10b). If the contour of integration appearing in Eq. (7a) for the modified integral representation of the propagated field is taken as the real frequency axis, then each of the field values given by Eq. (13) may be shown [37] to be precisely the same value as that obtained from Eq. (7a) with a quadratic approximation of the modified phase function about the respective real frequency value at which the real part $X_M(\omega_r)$ of the modified phase function attains one of its two local maxima along the positive real frequency axis. This point is, in general, different from the point $\omega=\omega_c$ at which the expansion in the quasimonochromatic approximation [27–36] is taken about, and approaches this point in the limit as $T\to\infty$ at fixed $z>0$.

IV. DISCUSSION

The transition from the ultrashort to the quasimonochromatic pulse regime is now illustrated through several examples. Consider first the case of an input ultrashort Gaussian-modulated cosine wave with initial pulse width $2T=0.2$ fsec and applied carrier frequency $\omega_c=5.75\times10^{16}$ sec^{-1}, which is near the upper end of the absorption band of the single resonance Lorentz model di-

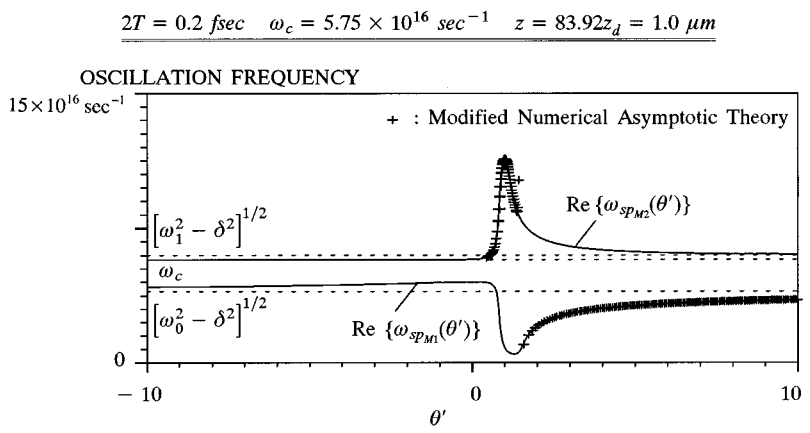

FIG. 2. The θ' evolution of the instantaneous frequency of oscillation of the propagated field of Fig. 1.

electric considered here [see the discussion following Eqs. (11a) and (11b)], at a propagation distance of $z = 83.92 z_d = 1.0$ μm, where z_d denotes the e^{-1} absorption depth at the carrier frequency ω_c. The input Gaussian envelope at the plane $z = 0$ is chosen to be centered at the time $t_0 = 15T$. The upper diagram in Fig. 1 illustrates the frequency dependence of $X_M(\omega_r)$, the real part of the modified complex phase function evaluated along the real frequency axis, as given by Eqs. (A12a)–(A12c). Notice that for a physically realizable input Gaussian pulse, $\omega_c > 0$ and the two local maxima of $X_M(\omega_r)$ that are located along the positive real frequency axis at ω_{mx_l}, $l = 1,2$, always dominate the remaining third local maximum that is situated along the negative real frequency axis at ω_{mx_3} [37]. As a consequence, particular attention may be focused on each of the two frequency intervals around the points ω_{mx_1} and ω_{mx_2}. The dynamical evolution in the complex ω plane of the five saddle points P_{Mk}, $k = 1,2,\ldots,5$ of the modified phase function $\Phi_M(\omega,\theta')$ as a function of θ' is illustrated in the middle diagram of Fig. 1. Notice that the two saddle points P_{M4} and P_{M5} approach the two left branch points ω_- and ω_-', respectively, while the two saddle points P_{M1} and P_{M2} approach the two right branch points ω_+ and ω_+', respectively, of the complex index of refraction $n(\omega)$ as θ' approaches $+\infty$. Moreover, the saddle point P_{M2} asymptotically approaches the vertical line $\omega = \omega_c$ from above as θ' tends to $-\infty$, while the saddle point P_{M3} asymptotically approaches the same line from below as θ' tends to $+\infty$. The first-order saddle point P_{M2} is the dominant relevant saddle point of the modified phase function $\Phi_M(\omega,\theta')$ for all $\theta' < 1.455$, its trajectory intersecting the real frequency axis at $\omega = \omega_{rc_{M2}} = 9.0261 \times 10^{16}$ sec^{-1} when $\theta' = \theta_{rc_{M2}} = 1.2831$. For all $\theta' > 1.455$, the first-order saddle point P_{M1} is the dominant relevant saddle point of $\Phi_M(\omega,\theta')$, its trajectory intersecting the positive real frequency axis at $\omega = \omega_{rc_{M1}} = 1.422 \times 10^{16}$ sec^{-1} when $\theta' = \theta_{rc_{M1}} = 1.6871$. The close agreement between the corresponding quantities ω_{mx_1} and $\omega_{rc_{M2}}$, as well as between the corresponding quantities ω_{mx_2} and $\omega_{rc_{M1}}$, is in complete agreement with the last part of proposition 2 of the preceding section.

The bottom diagram in Fig. 1 illustrates the dynamical evolution of the propagated field $A(z,t)$ that was computed using the modified asymptotic description presented in Eqs. (12a) and (12b). It is clearly seen that the input ultrashort Gaussian-modulated envelope pulse has evolved into two Gaussian-shaped pulse components, the first pulse component containing high-frequency oscillations while the second pulse component contains low-frequency oscillations. The first pulse component $A_s(z,t) = A_{M2}(z,t)$ is recognized as a generalized Sommerfeld precursor field [24,25] and is due to the asymptotic contribution of the first-order saddle point P_{M2}. This generalized Sommerfeld precursor field is the dominant pulse component of the propagated field $A(z,t)$ for all $\theta' < 1.455$, which is the space-time interval when P_{M2} is the dominant relevant saddle point of the modified phase function $\Phi_M(\omega,\theta')$. The peak in the envelope of $A_S(z,t)$ occurs at the space-time point $\theta = \theta_{p_S} = \theta_{p_{M2}} = 1.256$, at which point the propagated field oscillates with the instantaneous angular frequency $\omega_1 = \omega_{p_S} = \omega_{p_{M2}} = 9.2669 \times 10^{16}$ sec^{-1}. For all $\theta' > 1.455$, the propagated field $A(z,t)$ is dominated by the second pulse component $A_B(z,t) = A_{M1}(z,t)$, which is recognized as a generalized Brillouin precursor field [24,25]. This pulse component is due to the asymptotic contribution of the first-order saddle point P_{M1}, which is the dominant relevant saddle point of the modified phase function $\Phi_M(\omega,\theta')$ over this space-time interval. The peak in the envelope of $A_B(z,t)$ occurs at the space-time point $\theta = \theta_{p_B} = \theta_{p_{M1}} = 1.6724$, at which point the propagated field oscillates with the instantaneous angular frequency $\omega_1 = \omega_{pb} = \omega_{p^{M1}} = 1.3534 \times 10^{16}$ sec^{-1}. Notice the close agreement between the numerical values of the following ordered pairs of quantities:

$$(\theta_{rc_{M2}}, \omega_{rc_{M2}}) \leftrightarrow (\theta_{p_{M2}}, \omega_{p_{M2}}),$$

$$(\theta_{rc_{M1}}, \omega_{rc_{M1}}) \leftrightarrow (\theta_{p_{M1}}, \omega_{p_{M1}}).$$

This agreement is in keeping with the first part of proposition 2 of the preceding section.

Figure 2 illustrates the θ' evolution of the instantaneous frequency of oscillation of the propagated field considered in Fig. 1. The data points indicated by the + symbols in the diagram were numerically determined from the dynamical field evolution as described by the modified asymptotic approach. The two solid curves in the figure depict the θ' dependence of the real parts of the saddle point locations for the two dominant relevant saddle points P_{M1} and P_{M2}, respectively. As the space-time parameter θ' increases over the domain $\theta' < 1.455$, the instantaneous oscillation fre-

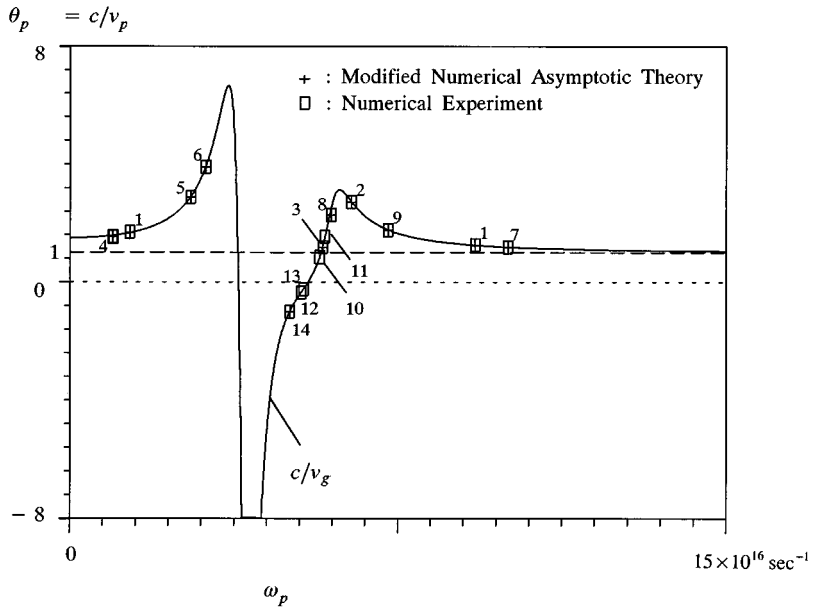

FIG. 3. Velocity of propagation of the peak amplitude point of each pulse component of the propagated field due to an input Gaussian pulse. The solid curve in the figure denotes the frequency dependence of the inverse relative group velocity $c/v_g(\omega_{p_k})$ evaluated at the instantaneous oscillation frequency ω_{p_k} of the propagated field component $A_{mk}(z,t)$. The indicated data values are for the following cases: 1, $\omega_c=5.75\times10^{16}$ sec^{-1}, $2T=0.20$ fsec, $z=83.92z_d=1.0$ μm; 2, $\omega_c=5.75\times10^{16}$ sec^{-1}, $2T=2.00$ fsec, $z=83.92z_d=1.0$ μm; 3, $\omega_c=5.75\times10^{16}$ sec^{-1}, $2T=20.0$ fsec, $z=83.92z_d=1.0$ μm; 4, $\omega_c=1.00\times10^{16}$ sec^{-1}, $2T=2.00$ fsec, $z=0.543z_d=1.0$ μm; 5, $\omega_c=3.1416\times10^{16}$ sec^{-1}, $2T=2.0$ fsec, $z=22.5z_d=1.0$ μm; 6, $\omega_c=4.00\times10^{16}$ sec^{-1}, $2T=2.00$ fsec, $z=266.6z_d=1.0$ μm; 7, $\omega_c=10.0\times10^{16}$ sec^{-1}, $2T=2.00$ fsec, $z=3.020z_d=1.0$ μm; 8, $\omega_c=5.75\times10^{16}$ sec^{-1}, $2T=2.00$ fsec, $z=8.392z_d=0.1$ μm; 9, $\omega_c=5.75\times10^{16}$ sec^{-1}, $2T=2.00$ fsec, $z=839.2z_d=10.0$ μm; 10, $\omega_c=5.625\times10^{16}$ sec^{-1}, $2T=5.0$ fsec, $z=19.96z_d=0.2$ μm; 11, $\omega_c=5.625\times10^{16}$ sec^{-1}, $2T=5.0$ fsec, $z=49.91z_d=0.5$ μm; 12, $\omega_c=5.25\times10^{16}$ sec^{-1}, $2T=10.0$ fsec, $z=58.05z_d=0.4$ μm; 13, $\omega_c=5.25\times10^{16}$ sec^{-1}, $2T=10.0$ fsec, $z=145.13z_d=1.0$ μm; 14, $\omega_c=5.00\times10^{16}$ sec^{-1}, $2T=20.0$ fsec, $z=176.1z_d=1.0$ μm.

quency values of the propagated field $A(z,t)$ are equal to those of its dominant first pulse component $A_S(z,t)=A_{M2}(z,t)$, and lie along the solid line depicting the θ' dependence of the real part of the saddle point location of P_{M2}, which is the dominant relevant saddle point of the modified phase function over this entire θ' domain; that is,

$$\omega_S(\theta')=\mathrm{Re}\{\omega_{P_{M2}}(\theta')\} \tag{14}$$

for all $\theta'<1.455$. Since the input carrier frequency ω_c is situated in the absorption band of the medium, and since $\mathrm{Re}\{\omega_{SP_{M2}}(\theta')\}$ approaches the upper end of the absorption band from above as $\theta'\to\infty$, then $\omega_s(\theta')>\omega_c$. For all increasing values of θ' over the space-time interval $\theta'>1.455$, the values of the instantaneous oscillation frequency of the propagated field $A(z,t)$ are equal to those of its now dominant second pulse component $A_B(z,t)=A_{M1}(z,t)$, and lie along the solid line depicting the θ' dependence of the real part of the saddle point location of P_{M1}, which is the dominant relevant saddle point of the modified phase function over this entire θ' domain; that is,

$$\omega_B(\theta')=\mathrm{Re}\{\omega_{SP_{M1}}(\theta')\} \tag{15}$$

for all $\theta'>1.455$. Since $\mathrm{Re}\{\omega_{SP_{M1}}(\theta')\}$ approaches the lower end of the absorption band from below as $\theta'\to\infty$, then $\omega_B(\theta')<\omega_c$. These results are in keeping with proposition 1 of the preceding section.

The frequency components of the propagated field considered in Figs. 1 and 2 that lie within the medium absorption band $\omega_0\leqslant\omega_r\leqslant\omega_1$ have been greatly attenuated at the chosen propagation distance and are practically absent from the propagated field structure. Since the input carrier frequency ω_c lies within the absorption band in this case, the propagated pulse spectrum evolves into two spectral component domains, one a high-frequency component domain that lies above the medium absorption band with a maximum at $\omega_r=\omega_{mx_1}$, the other a low-frequency component domain that lies below the medium absorption band with a maximum at $\omega_1=\omega_{mx_2}$. The first pulse component $A_{M2}(z,t)$ of the propagated field $A(z,t)$ is then due to the propagated spectral components in the high-frequency band so that the field at the peak in the envelope of $A_{M2}(z,t)$ oscillates at the angular frequency $\omega_{p_{M2}}=\omega_{rc_{M2}}=\omega_{mx_1}$ of the dominant spectral component in this frequency band. The second pulse component $A_{M1}(z,t)$ of the propagated field $A(z,t)$ is due to the propagated spectral components in the low-frequency band so that the field at the peak in the envelope of $A_{M1}(z,t)$ oscillates at the angular frequency $\omega_{p_{M1}}=\omega_{rc_{M1}}=\omega_{mx_2}$ of the dominant spectral component in this frequency band.

Consider now the velocity of propagation $v_{p_{Ml}}$, $l=1,2$, of the peak in the envelope of each dominant pulse component $A_{Ml}(z,t)$ of the propagated field $A(z,t)$ due to an input Gaussian pulse of arbitrary initial pulse width. The numerical value of the space-time point $\theta_{p_{Ml}}=c/v_{p_{Ml}}$ at which the peak

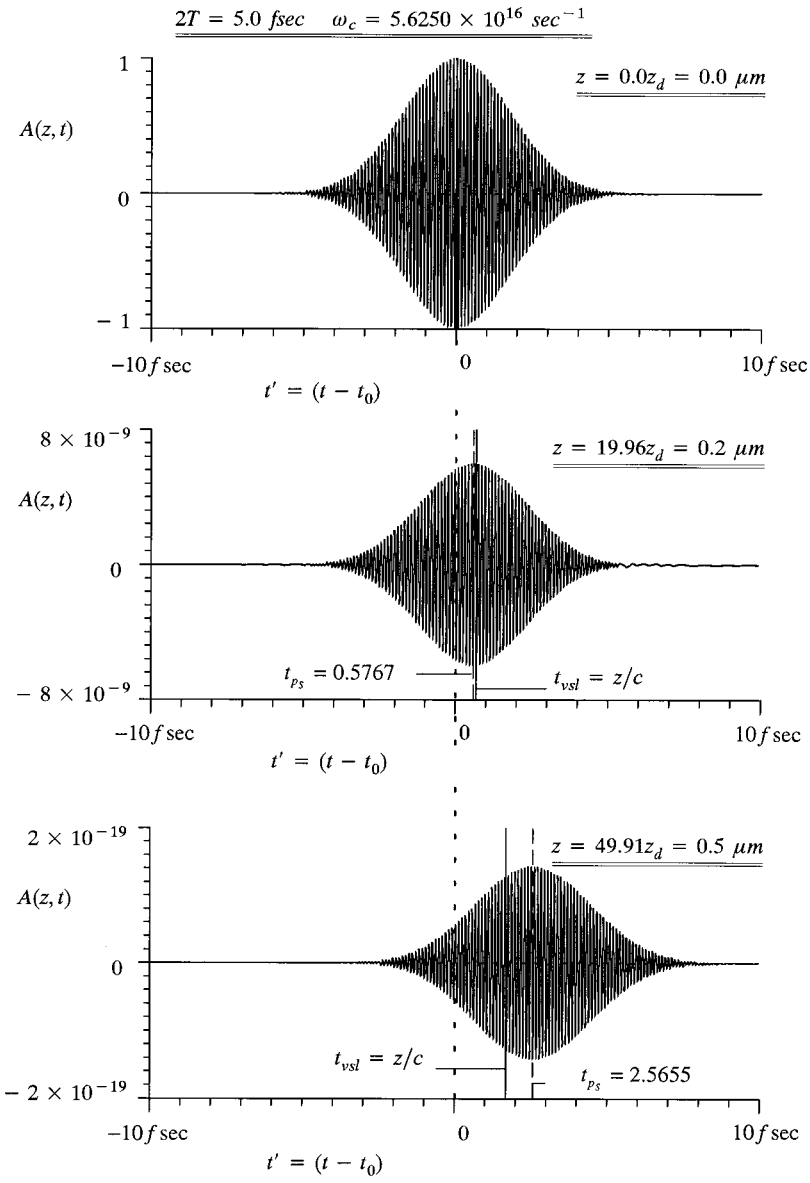

FIG. 4. Numerically determined dynamical field evolution due to an input unit-amplitude Gaussian-envelope-modulated cosine wave with initial pulse width $2T=5.0$ fsec and carrier frequency $\omega_c=5.625\times10^{16}$ sec^{-1} at the input plane (top diagram) and at two increasing propagation distances z in a single resonance Lorentz model dielectric. The horizontal axis in each diagram denotes the retarded time with $t_0=15T$. In each of the bottom two diagrams, the solid vertical line marks the instant of time $t'=z/c$ when the peak amplitude of the propagated pulse would have arrived at that propagation distance if it had traveled with the speed of light in vacuum, while the vertical dashed line marks the actual instant of time $t'=t_{p_S}$ when the peak amplitude in the propagated pulse arrives at that propagation distance z. The middle diagram corresponds to the superluminal velocity case 10 and the bottom diagram to the subluminal velocity case 11 depicted in Fig. 3.

in the envelope of each dominant pulse component of $A(z,t)$ occurs is plotted in Fig. 3 at the corresponding value of the instantaneous frequency of oscillation $\omega_{p_{MI}}$ at which that envelope peak occurs for a wide variety of input pulses. The squares in the figure denote the values of the results obtained from numerical experiments, while the crosses denote the corresponding values determined from the results described by the modified asymptotic approach. Both sets of values are exactly located on the solid curve in the figure which describes the frequency dependence of the relative inverse group velocity $c/v_g(\omega_r)$ for the single resonance Lorentz model dielectric considered here. These results are in keeping with proposition 3 of the preceding section.

Of particular interest in Fig. 3 is case 10 which shows that the peak velocity $v_{p_{MI}}$, may become larger than the speed of light in vacuum, as well as cases 12–14 which show that $v_{p_{MI}}$, may even become negative. These cases clearly warrant further, more detailed consideration, which is now given. Consider first the dynamical field evolution due to an input Gaussian-envelope-modulated cosine wave with initial pulse width $2T=5.0$ fsec and applied carrier frequency $\omega_c=5.625\times10^{16}$ sec^{-1}. The top diagram in Fig. 4 illustrates the initial field evolution at the input observation plane at $z=0$, whereas the bottom two diagrams illustrate the dynamical field evolution of the resultant propagated field at two increasing propagation distances in the single resonance Lorentz model dielectric considered in this paper. In each of these diagrams, the horizontal axis represents the retarded time $t'=(t-t_0)$. In each of the bottom two diagrams of this figure, the vertical dashed line denotes the retarded instant of time $t'=t_{p_S}$ at which the peak in the envelope of the single dominant, Gaussian-shaped pulse component $A_S(z,t)$ of $A(z,t)$ arrives at that corresponding propagation distance, while the solid vertical line denotes the retarded instant of time $t'=t_{vsl}=z/c$ when this envelope peak would have arrived at the corresponding propagation distance if it had traveled at the speed of light in vacuum. If $t_{p_s}<0$, then the envelope peak of $A(z,t)$ propagates with a negative velocity; if $0<t_{p_s}<t_{vsl}$, then the envelope peak propagates with a velocity that is greater than the speed of light in vacuum (i.e.,

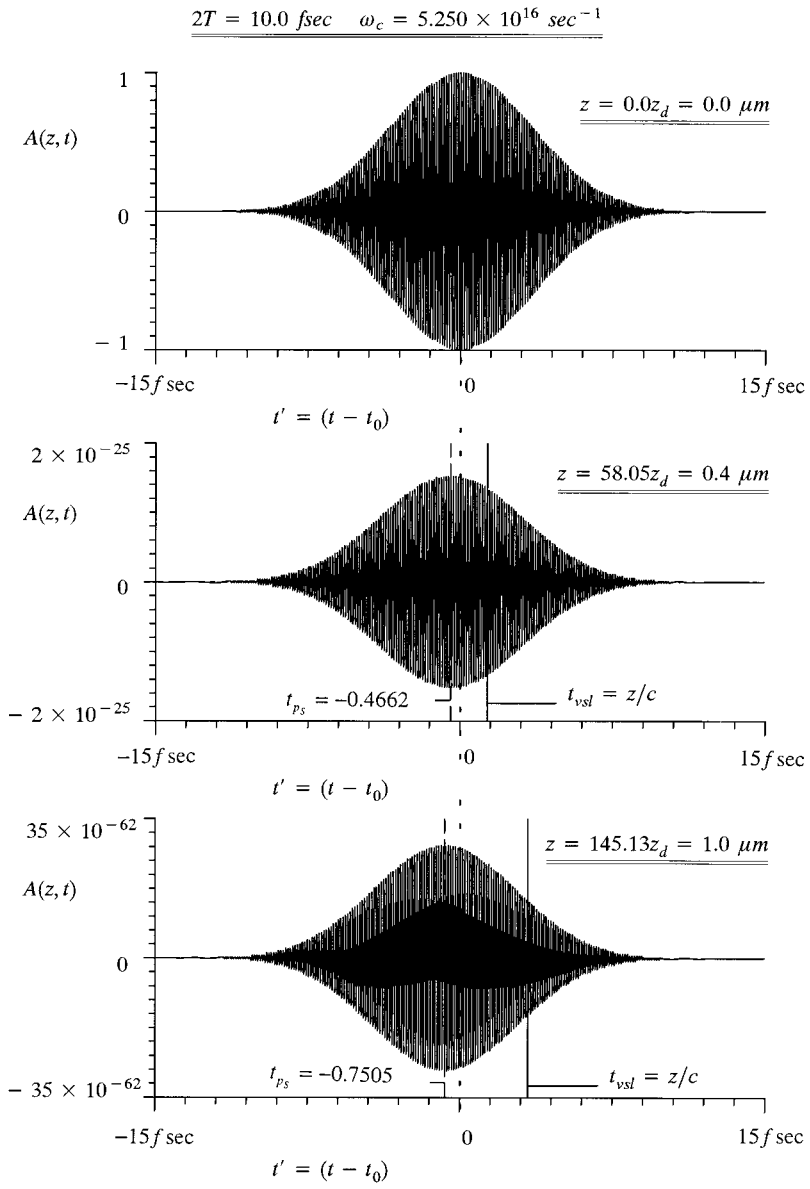

FIG. 5. Numerically determined dynamical field evolution due to an input unit-amplitude Gaussian-envelope-modulated cosine wave with initial pulse width $2T=10.0$ fsec and carrier frequency $\omega_c=5.25\times10^{16}$ sec^{-1} at the input plane (top diagram) and at two increasing propagation distances z in a single resonance Lorentz model dielectric. The horizontal axis in each diagram denotes the retarded time with $t_0=15T$. In each of the bottom two diagrams, the solid vertical line marks the instant of time $t=z/c$ when the peak amplitude of the propagated pulse would have arrived at that propagation distance if it had traveled with the speed of light in vacuum, while the vertical dashed line marks the actual instant of time $t'=t_{p_S}$ when the peak amplitude in the propagated pulse arrives at that propagation distance z. The middle diagram corresponds to the negative velocity case 12 and the bottom diagram to the negative velocity case 13 depicted in Fig. 3.

with a superluminal velocity); while if $t_{p_s}>t_{vsl}$, then the envelope peak propagates with a velocity that is smaller than the speed of light in vacuum (i.e., with a subluminal velocity). Notice that if $t_{p_s}=0$, then the peak in the envelope of $A(z,t)$ would have propagated with an infinite velocity. The dispersive action of the single resonance Lorentz model dielectric on the input Gaussian pulse produces the superluminal velocity of the peak in the envelope of the propagated field $A(z,t)$ at a sufficiently small propagation distance, as illustrated in the middle diagram of Fig. 4 with the corresponding case 10 data point in Fig. 3. This same envelope peak slows down to a subluminal velocity as the propagation distance increases, as illustrated in the bottom diagram of Fig. 4 with the corresponding case 11 data point in Fig. 3, due to the same dispersive action. For sufficiently small propagation distances, this envelope peak occurs at an angular frequency at which the group velocity is superluminal; for the case illustrated in the middle diagram of Fig. 4, the field at the peak in the envelope of $A(z,t)$ oscillates with the instantaneous angular frequency $\omega_{p_S}\cong5.71\times10^{16}$ sec^{-1} and it propagates with the classical group velocity $v_{p_S}=v_g(\omega_{p_S})\cong1.16c$ at this frequency value. However, this frequency component is also highly attenuated by the lossy, dispersive medium, so that as the pulse continues to propagate through the medium, the envelope peak shifts toward those frequency values that have less attenuation associated with them, and accordingly propagate with subluminal velocities; for the case illustrated in the bottom diagram of Fig. 4, the instantaneous frequency of oscillation of the envelope peak of the propagated field $A(z,t)$ has shifted to the higher-frequency value $\omega_{p_S}\cong5.83\times10^{16}$ sec^{-1}, and this envelope peak propagates with the classical group velocity $v_{p_S}=v_g(\omega_{p_S})\cong0.65c$ at this frequency. As the propagation distance increases, the instantaneous oscillation frequency evolves out of the absorption band and the observed pulse dynamics evolve toward the energy velocity description [40–42] which is valid in the mature dispersion regime.

The other situation of special interest is presented in Fig. 5, which depicts the dynamical field evolution due to an input Gaussian-envelope-modulated cosine wave with initial pulse width $2T=10$ fsec and applied carrier frequency $\omega_c=5.25\times10^{16}$ sec^{-1}. The dynamical field evolution of the

input pulse at the plane $z=0$ is illustrated in the upper diagram of Fig. 5, and the dynamical evolution of the resultant propagated field at the two propagation distances $z=0.4$ and 1.0 μm in the single resonance Lorentz medium considered here are illustrated in the middle and bottom diagrams, respectively, of this figure. It is clearly seen in this figure sequence that at a sufficiently small propagation distance, the peak of the envelope of the single dominant, Gaussian-shaped pulse component $A_S(z,t)$ of the propagated field $A(z,t)$ propagates with a negative velocity, as seen in the middle diagram of Fig. 5, which corresponds to the case 12 data point in Fig. 3. The velocity v_{p_S} at which the envelope peak of $A(z,t)$ propagates remains negative while its absolute value increases as the propagation distance is slightly increased, as seen in the bottom diagram of Fig. 5, which corresponds to the case 13 data point in Fig. 3. This phenomenon is directly attributed to the action of the material dispersion on the frequency components of the pulse as it propagates through the lossy, dispersive medium. In this case, the temporal spectrum of the input Gaussian pulse is sharply peaked around the carrier frequency ω_c which lies in the upper half of the medium absorption band. As the propagation distance increases, the low-frequency components that are present in the input pulse spectrum are attenuated at a larger rate than are the high-frequency components. Consequently, as the propagation distance increases, the propagated pulse spectrum becomes dominated by an increasingly higher-frequency component, and the peak in the envelope of the propagated field $A(z,t)$ propagates with the group velocity at this frequency value. At the small propagation distance considered in the middle diagram of Fig. 5, the dominant spectral component of the propagated field occurs at the angular frequency value $\omega_{p_S}\cong 5.29\times 10^{16}$ sec$^{-1}>\omega_c$, which still lies within the absorption band of the medium, and the envelope peak of $A(z,t)$ propagates with the classical group velocity $v_{p_S}=v_g(\omega_{p_S})\cong -2.86c$ at this frequency value. At the slightly larger propagation distance considered in the bottom diagram of Fig. 5, the dominant spectral component of the propagated pulse has been shifted further to the higher-frequency value $\omega_{p_s}\cong 5.35\times 10^{16}$ sec^{-1} and the envelope peak of $A(z,t)$ now propagates with the classical group velocity $v_{p_S}=v_g(\omega_{p_S})\cong -4.45c$ at this higher angular frequency. This observed trend that the group velocity of the envelope peak of $A(z,t)$ becomes increasingly negative as the propagation distance increases remains intact as the propagation distance z is increased further; however, the overall field amplitude also rapidly attenuates to zero in this case. Again, as the propagation distance increases into the mature dispersion regime, the pulse dynamics evolve toward the energy velocity description [40–42].

Similar analytical and numerical results have also been reported by Garrett and McCumber [27], who argue that, for input Gaussian-modulated harmonic wave with no true beginning or end with carrier frequency in the anomalous dispersion region of a Lorentz-type medium, the superluminal and negative velocity dynamics of the envelope peak of the propagated pulse are both due to the action of the dispersive medium on the weak early frequency components of the input Gaussian envelope. Moreover, in his analytical investigations of the propagation of an input Gaussian pulse through a resonant dielectric comprised of a homogeneous distribution of two-level atoms embedded in a nondispersive host medium, Crisp [29] utilized the semiclassical theory formalism to show that both the superluminal and the negative velocity dynamics of the envelope peak of the propagated pulse are due to the finite response time of the resonant atoms on the input Gaussian pulse. Notice also that both superluminal and negative group velocities in both attenuative and amplifying media have been observed experimentally [43–45]. The attenuative medium results are in agreement with the results of the generalized asymptotic description presented in this paper at small propagation distances. However, our analysis also clearly shows that the generalized asymptotic description evolves into the energy velocity description as the propagation distance increases into the mature dispersion regime. This asymptotic description of Gaussian pulse propagation in a lossy, dispersive medium, which is uniform in the initial pulse width, also provides a clear description of the transition from the ultrashort pulse limit $T\leqslant 1/\delta$, in which the propagated pulse separates into a generalized Sommerfeld precursor pulse component and a generalized Brillouin precursor pulse component, [24] to the slowly varying envelope (or quasimonochromatic) regime $T>1/\delta$ in which the propagated field dynamics become dominated by a single one of these two pulse components. Notice that for the numerical examples presented in this paper, the transition between the ultrashort and slowly varying envelope regimes occurs at the characteristic relaxation time $1/\delta=0.357$ fsec of this highly absorbing Lorentz model medium. As a point of comparison, about the infrared absorption line in triply distilled H_2O at $\omega=1.13\times 10^{14}$ sec^{-1}, $\delta=2.7\times 10^{13}$ sec^{-1} so that $1/\delta=37$ fsec.

ACKNOWLEDGMENT

The research presented in this paper was supported by the Applied Mathematics Division of the United States Air Force Office of Scientific Research under Grant Nos. F49620-92-J-0206 and F49620-94-1-0430.

APPENDIX

From Eqs. (12a) and (12b), if P_{Ml} is the dominant relevant saddle point of the modified complex phase function $\Phi_M(\omega,\theta')$ in the θ' interval $\Delta\theta_{Ml}$, i.e., the relevant saddle point with the least exponential decay associated with it for all $\theta'\in\Delta\theta_{Ml}$, then the asymptotic contribution $A_{Ml}(z,t)$ is the dominant pulse component of the propagated field $A(z,t)$ in this θ' domain. At each saddle point P_{Ml} of the modified complex phase function $\Phi_M(\omega,\theta')$ the following pair of relations are satisfied:

$$\left.\frac{\partial X_M(\omega_r,\omega_i,\theta')}{\partial\omega_r}\right|_{\omega=\omega_{P_{Ml}}}=\left.\frac{\partial Y_M(\omega_r,\omega_i,\theta')}{\partial\omega_i}\right|_{\omega=\omega_{P_{Ml}}}=0, \tag{A1a}$$

$$\left.\frac{\partial X_M(\omega_r,\omega_i,\theta')}{\partial\omega_i}\right|_{\omega=\omega_{P_{Ml}}}=-\left.\frac{\partial Y_M(\omega_r,\omega_i,\theta')}{\partial\omega_r}\right|_{\omega=\omega_{P_{Ml}}}=0, \tag{A1b}$$

and also

$$\left.\frac{d^2\Phi_M(\omega,\theta')}{d\omega^2}\right|_{\omega=\omega_{P_{Ml}}} = \left|\frac{d^2\Phi_M(\omega_{P_{Ml}},\theta')}{d\omega^2}\right| \times \exp\left\{ i \arg\left[\frac{d^2\Phi_M(\omega_{P_{Ml}},\theta')}{d\omega^2}\right]\right\} \neq 0. \tag{A2}$$

Here, $X_M = \mathrm{Re}\{\Phi_M\}$, $Y_M = \mathrm{Im}\{\Phi_M\}$, and $\omega_r = \mathrm{Re}\{\omega\}$, $\omega_i = \mathrm{Im}\{\omega\}$, and the proper branch of the argument of the term appearing in Eq. (A2) is specified during the implementation of the modified asymptotic approach [10,11,16,37].

The instantaneous angular frequency of oscillation of $A_{Ml}(z,t)$, as well as that of $A(z,t)$, over the θ' interval $\Delta\theta_{Ml}$ is obtained from the time derivative of the oscillatory phase term appearing in Eq. (12b) as [8,16,26]

$$\omega_{I_{Ml}}(\theta') = -\frac{d}{dt}\left\{\frac{z}{c} Y_M(\omega^r_{P_{Ml}}(\theta'),\omega^i_{P_{Ml}}(\theta'),\theta') - \frac{1}{2}\left[\arg\left(\frac{d^2\Phi_M(\omega_{P_{Ml}}(\theta'),\theta')}{d\omega^2}\right)+\pi\right]\right\}, \tag{A3}$$

where $\omega^r_{P_{Ml}}(\theta') = \mathrm{Re}\{\omega_{P_{Ml}}(\theta')\}$ and $\omega^i_{P_{Ml}}(\theta') = \mathrm{Im}\{\omega_{P_{Ml}}(\theta')\}$ are the real and imaginary parts of the relevant saddle point location, respectively. Application of the chain rule and Eqs. (A1a) and (A1b) to Eq. (A3) then yields [37]

$$\omega_{I_{Ml}}(\theta') = \mathrm{Re}\{\omega_{P_{Ml}}(\theta')\} + \Delta_{1Ml}(\theta') \sim \mathrm{Re}\{\omega_{P_{Ml}}(\theta')\}, \tag{A4}$$

where the final expression is asymptotically valid as $z\to+\infty$. Here the term $\Delta_{1Ml}(\theta')$ is given by

$$\Delta_{1Ml}(\theta') = \frac{1}{2}\frac{d}{dt}\left\{\arg\left[\frac{d^2\Phi_M(\omega_{P_{Ml}}(\theta'),\theta')}{d\omega^2}\right]\right\} = O(z^{-1}) \tag{A5}$$

as $z\to+\infty$, so that this term is asymptotically negligible in comparison to the first term on the right-hand side of Eq. (A4), as indicated in the final expression.

In any particular θ' interval $\Delta\theta_{Ml}$, the stationary points of the envelope of the dominant field component $A_{Ml}(z,t)$, as well as those of the envelope of the propagated field $A(z,t)$ over that θ' interval, are given by the solutions of the equation

$$\frac{d}{dt}\left\{\left|\frac{d^2\Phi_M(\omega_{P_{Ml}}(\theta'),\theta')}{d\omega^2}\right|^{-1/2} \times \exp\left[\frac{z}{c} X_M(\omega^r_{P_{Ml}}(\theta'),\omega^i_{P_{Ml}}(\theta'),\theta')\right]\right\} = 0, \tag{A6}$$

which was obtained from Eq. (12b). Application of the chain rule and use of Eqs. (A1a) and (A1b) in Eq. (A6) then yields [37]

$$\left\{\left|\frac{d^2\Phi_M(\omega_{P_{Ml}},\theta')}{d\omega^2}\right|^{-1/2} \exp\left[\frac{z}{c} X_M(\omega^r_{P_{Ml}},\omega^i_{P_{Ml}},\theta')\right]\right\} \times\{-\Delta_{2Ml}(\theta') + \mathrm{Im}[\omega_{P_{Ml}}(\theta')]\} = 0, \tag{A7}$$

which is satisfied when the condition

$$\mathrm{Im}\{\omega_{P_{Ml}}(\theta')\} = \Delta_{2Ml}(\theta') \tag{A8}$$

is satisfied, where

$$\Delta_{2Ml}(\theta') = \frac{1}{4}\frac{d}{dt}\left\{\ln\left[\left|\frac{d^2}{d\omega^2}\Phi_M(\omega_{P_{Ml}}(\theta'),\theta')\right|^2\right]\right\} = O(z^{-1}) \tag{A9}$$

as $z\to+\infty$, so that this quantity is asymptotically negligible in comparison to $\mathrm{Re}\{\omega_{P_{Ml}}(\theta')\}$. It follows from Eq. (A6) that such a stationary point is a maximum (minimum) when the time derivative of the quantity appearing inside the second set of brackets $\{\}$ on the left-hand side of Eq. (A7) is negative (positive).

Let $\theta_{rc_{Ml}}$ denote the space-time parameter value in the interval $\Delta\theta_{Ml}$ when the trajectory followed in the complex ω plane by the dominant relevant saddle point P_{Ml} of the modified phase function $\Phi_M(\omega,\theta')$ intersects the real frequency axis at the real frequency value denoted by $\omega_{rc_{Ml}} = \omega_{P_{Ml}}(\theta_{rc_{Ml}})$. Moreover, let $\theta_{p_{Ml}}$ denote the space-time point in the same space-time interval $\Delta\theta_{Ml}$ when the envelope of the dominant pulse component $A_{Ml}(z,t)$ of the propagated field $A(z,t)$ attains its corresponding stationary point whose instantaneous frequency of oscillation is denoted by $\omega_{p_{Ml}}$. From Eq. (A4) and Eqs. (A6)–(A9) one has that

$$\theta_{p_{Ml}} = \theta_{rc_{Ml}}, \tag{A10a}$$

and

$$\omega_{p_{Ml}} = \omega_{rc_{Ml}} = \omega_{P_{Ml}}(\theta_{p_{Ml}}) = \omega_{P_{Ml}}(\theta_{rc_{Ml}}). \tag{A10b}$$

From Eqs. (7c) and (13a) it may be shown that [37]

$$\left.\frac{\partial X_M(\omega_r,\omega_i,\theta')}{\partial\omega_r}\right|_{\omega=\omega_{p_{Ml}}} = \left.\frac{\partial X_M(\omega_r)}{\partial\omega_r}\right|_{\omega=\omega_{p_{Ml}}} = 0, \tag{A11}$$

where

$$X_M(\omega_r) = \mathrm{Re}\{\Phi_M(\omega_r,\omega_i,\theta')|_{\omega_i=0}\} = X(\omega_r) + X_f(\omega_r) \tag{A12a}$$

denotes the real part of the modified phase function evaluated along the real frequency axis, with

$$X(\omega_r) = \mathrm{Re}\{\phi(\omega_r,\omega_i,\theta')|_{\omega_i=0}\} = -\omega_r n_i(\omega_r) \tag{A12b}$$

being the real part of the classical phase function evaluated along the real frequency axis, and with

$$X_f(\omega_r)=\mathrm{Re}\{\Phi_f(\omega_r,\omega_i)|_{\omega_i=0}\}=-\frac{cT^2}{4z}(\omega_r-\omega_c)^2 \tag{A12c}$$

being the real part of the phase term that is contributed by the spectrum of the input Gaussian pulse-modulated sine wave with carrier frequency ω_c evaluated along the real frequency axis. Substitution of Eqs. (A12a)–(A12c) in Eq. (A11) then yields [37]

$$\frac{\partial}{\partial\omega_r}[\alpha(\omega_r)]_{\omega_r=\omega_{p_{Ml}}}=-\frac{T^2}{2z}(\omega_{p_{Ml}}-\omega_c), \tag{A13}$$

where [see Eq. (6)]

$$\alpha(\omega_r)=\frac{\omega_r}{c}n_i(\omega_r) \tag{A14}$$

denotes the coefficient of absorption of the dispersive medium with complex index of refraction $n(\omega)=n_r(\omega)+in_i(\omega)$.

The value $\theta_{p_{Ml}}\in\Delta\theta_{Ml}$ when the envelope of $A_{Ml}(z,t)$ attains a stationary point may be obtained from Eq. (A1b) with the result [37]

$$\theta_{p_{Ml}}=\frac{\partial}{\partial\omega_r}[\omega_r n_r(\omega_r)]_{\omega_r=\omega_{p_{Ml}}}, \tag{A15}$$

where $n_r(\omega)$ denotes the real part of the complex index of refraction. This stationary point then propagates with the velocity

$$v_{p_{Ml}}=\frac{c}{\theta_{p_{Ml}}}=v_g(\omega_{p_{Ml}}), \tag{A16a}$$

where

$$v_g(\omega_{p_{Ml}})=\left\{\frac{\partial}{\partial\omega_r}\left[\frac{\omega_r}{c}n_r(\omega_r)\right]_{\omega_r=\omega_{p_{Ml}}}\right\}^{-1} \tag{A16b}$$

is the classical group velocity evaluated at the angular frequency $\omega_{p_{Ml}}=\omega_{rc_{Ml}}=\omega_{P_{Ml}}(\theta_{p_{Ml}})$ at which the dominant relevant saddle point P_{Ml} of the modified phase function $\Phi_M(\omega,\theta')$ intersects the real frequency axis [see Eqs. (A10a) and (A10b)].

[1] D. H. Auston, K. P. Cheung, J. A. Valdmanis, and D. A. Kleinman, Phys. Rev. Lett. **53**, 1555 (1984).
[2] R. L. Fork, C. H. Brito Cruz, P. C. Becker, and C. V. Shank, Opt. Lett. **12**, 483 (1987).
[3] J. D. Jackson, *Classical Electrodynamics*, 2nd ed. (Wiley, New York, 1975), Chap. 7.
[4] L. Allen and J. H. Eberly, *Optical Resonance and Two-Level Atoms* (Wiley, New York, 1975).
[5] S. A. Akhmanov, V. A. Vysloukh, and A. S. Chirkin, *Optics of Femtosecond Laser Pulses* (AIP, New York, 1992).
[6] Y. R. Shen, *The Principles of Nonlinear Optics* (Wiley, New York, 1984).
[7] P. N. Butcher and D. Cotter, *The Elements of Nonlinear Optics* (Cambridge University Press, Cambridge, England, 1990).
[8] L. Brillouin, *Wave Propagation and Group Velocity* (Academic, New York, 1960).
[9] E. T. Copson, *Asymptotic Expansions* (Cambridge University Press, Cambridge, England, 1971).
[10] F. W. J. Olver, *Asymptotics and Special Functions* (Academic, New York, 1974).
[11] F. W. J. Olver, SIAM Rev. **12**, 228 (1970).
[12] R. A. Handelsman and N. Bleistein, Arch. Ration. Mech. Anal. **35**, 267 (1969).
[13] C. Chester, B. Friedman, and F. Ursell, Proc. Cambridge Philos. Soc. **53**, 599 (1957).
[14] N. Bleistein, Commun. Pure Appl. Math. **19**, 353 (1966).
[15] N. Bleistein, J. Math. Mech. **17**, 533 (1967).
[16] K. E. Oughstun and G. C. Sherman, J. Opt. Soc. Am. B **5**, 817 (1988).
[17] K. E. Oughstun and G. C. Sherman, J. Opt. Soc. Am. A **6**, 1394 (1989).
[18] K. E. Oughstun, Proc. IEEE **79**, 1379 (1991).
[19] S. Shen and K. E. Oughstun, J. Opt. Soc. Am. B **6**, 948 (1989).
[20] P. Wyns, D. P. Foty, and K. E. Oughstun, J. Opt. Soc. Am. A **6**, 1421 (1989).
[21] K. E. Oughstun, P. Wyns, and D. P. Foty, J. Opt. Soc. Am. A **6**, 1430 (1989).
[22] R. M. Joseph, S. C. Hagness, and A. Taflove, Opt. Lett. **16**, 1412 (1991).
[23] K. E. Oughstun and G. C. Sherman, Phys. Rev. A **41**, 6090 (1990).
[24] K. E. Oughstun and J. E. K. Laurens, Radio Sci. **26**, 245 (1991).
[25] C. M. Balictsis and K. E. Oughstun, Phys. Rev. E **47**, 3645 (1993).
[26] L. B. Felsen, In *Transient Electromagnetic Fields*, edited by L. B. Felsen (Springer-Verlag, New York, 1976), Chap. 1. See also the references included therein.
[27] C. G. B. Garrett and D. E. McCumber, Phys. Rev. A **1**, 305 (1970).
[28] M. D. Crisp, Phys. Rev. A **1**, 1604 (1970).
[29] M. D. Crisp, Phys. Rev. A **4**, 2104 (1971).
[30] J. Jones, Am. J. Phys. **42**, 43 (1974).
[31] D. Anderson, J. Askne, and M. Lisak, Phys. Rev. A **12**, 1546 (1975).
[32] D. Anderson and M. Lisak, Phys. Rev. A **35**, 184 (1987).
[33] N. D. Hoc, I. M. Besieris, and M. E. Sockell, IEEE Trans. Antennas Propag. **AP-33**, 1237 (1985).
[34] E. Varoquaux, G. A. Williams, and O. Avenel, Phys. Rev. B **34**, 7617 (1986).
[35] I. P. Christov, IEEE J. Quantum Electron. **QE-24**, 1548 (1988).
[36] I. P. Christov, in *Progress in Optics*, edited by E. Wolf (Elsevier, Amsterdam, 1991), Vol. XXIX.

[37] C. M. Balictsis, Ph. D. dissertation, University of Vermont, 1994.
[38] K. E. Oughstun, J. E. K. Laurens, and C. M. Balictsis, in *Ultra-Wideband, Short-Pulse Electromagnetics*, edited by H. L. Bertoni, L. Carin, and L. B. Felsen (Plenum, New York, 1993).
[39] C. M. Balictsis and K. E. Oughstun, in *Ultra-Wideband, Short-Pulse Electromagnetics 2*, edited by H. L. Bertoni, L. Carin, L. B. Felsen, and S. V. Pillai (Plenum, New York, 1995).
[40] K. E. Oughstun and G. C. Sherman, *Electromagnetic Pulse Propagation in Causal Dielectrics* (Springer-Verlag, Berlin, 1994).
[41] G. C. Sherman and K. E. Oughstun, J. Opt. Soc. Am. B **12**, 229 (1995); see also Phys. Rev. Lett. **47**, 1451 (1981).
[42] K. E. Oughstun and C. M. Balictsis, Phys. Rev. Lett. **77**, 2210 (1996).
[43] L. Casperson and A. Yariv, Phys. Rev. Lett. **26**, 293 (1971).
[44] S. Chu and S. Wong, Phys. Rev. Lett. **48**, 738 (1982).
[45] A. Katz and R. R. Alfano, Phys. Rev. Lett. **49**, 1292 (1982).